

NLO BFKL AT WORK: THE ELECTROPRODUCTION OF TWO LIGHT VECTOR MESONS*

DMITRY YU. IVANOV

Sobolev Institute of Mathematics, 630090 Novosibirsk, Russia

ALESSANDRO PAPA

Dipartimento di Fisica, Università della Calabria
and Istituto Nazionale di Fisica Nucleare, Gruppo collegato di Cosenza
87036 Arcavacata di Rende, Cosenza, Italy

(Received May 12, 2008)

The forward electroproduction of two light vector mesons is the first example of a collision process between strongly interacting colorless particles for which the amplitude can be written completely within perturbative QCD in the Regge limit with next-to-leading accuracy. This amplitude can be written as a convolution of two impact factors for the virtual photon to light vector meson transition with the BFKL Green's function. In this lecture we first describe how the relevant impact factor is calculated, then we perform the convolution with the BFKL Green's function and illustrate the numerical procedure to obtain a well-behaved amplitude.

PACS numbers: 12.38.Bx, 13.60.Le, 11.55.Jy

1. Introduction

In the BFKL approach [1], both in the leading logarithmic approximation (LLA), which means resummation of leading energy logarithms, all terms $(\alpha_s \ln(s))^n$, and in the next-to-leading approximation (NLA), which means resummation of all terms $\alpha_s(\alpha_s \ln(s))^n$, the (imaginary part of the) amplitude for a large- s hard collision process can be written as the convolution of the Green's function of two interacting Reggeized gluons with the impact factors of the colliding particles (see, for example, Fig. 1).

The Green's function is determined through the BFKL equation. The NLA singlet kernel of the BFKL equation has been achieved in the forward case [2], after the long program of calculation of the NLA corrections [3]

* Presented by A. Papa at the School on QCD, Low x Physics, Saturation and Diffraction, Copanello, Calabria, Italy, July 1–14, 2007.

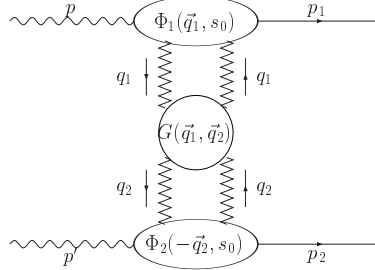


Fig. 1. Schematic representation of the amplitude for the $\gamma^*(p) \gamma^*(p') \rightarrow V(p_1) V(p_2)$ forward scattering.

(for a review, see Ref. [4]). For the non-forward case the ingredients to the NLA BFKL kernel have been known since a few years for the color octet representation in the t -channel [5]. This color representation is very important for the check of consistency of the s -channel unitarity with the gluon reggeization, *i.e.* for the “bootstrap” [6, 7]. Recently there was completed also the calculation of the non-forward NLA BFKL kernel in the singlet color representation, *i.e.* in the Pomeron channel, relevant for physical applications [8].

On the other side, NLA impact factors have been calculated for colliding partons [9, 10] and for forward jet production [11]. Among the impact factors for transitions between colorless objects, the most important one from the phenomenological point of view is certainly the impact factor for the virtual photon to virtual photon transition, *i.e.* the $\gamma^* \rightarrow \gamma^*$ impact factor, since it would open the way to predictions of the $\gamma^* \gamma^*$ total cross section. Its calculation is rather complicated and it was completed after year-long efforts [12–14].

A considerable simplification can be gained if one considers instead the impact factor for the transition from a virtual photon γ^* to a light neutral vector meson $V = \rho^0, \omega, \phi$. In this case, indeed, a close analytical expression can be achieved in the NLA, up to contributions suppressed as inverse powers of the photon virtuality [15]. In particular, it turns out that (a) the dominant helicity amplitude is that for the transition from longitudinally polarized virtual photon to longitudinally polarized vector meson; (b) the impact factor, both in the LLA and in the NLA, factorizes into the convolution of a hard scattering amplitude, calculable in perturbative QCD, and a meson twist-2 distribution amplitude [15].

The knowledge of the $\gamma^* \rightarrow V$ impact factor allows for the first time to determine completely within perturbative QCD and with NLA accuracy the amplitude of a physical process, the $\gamma^* \gamma^* \rightarrow VV$ reaction [16, 17]. This possibility is interesting first of all for theoretical reasons, since it can shed

light on the role and the optimal choice of the energy scales entering the BFKL approach. Moreover, it can be used as a test-ground for comparisons with approaches different from BFKL, such as DGLAP, and with possible next-to-leading order extensions of phenomenological models, such as color dipole and k_t -factorization. But it could be interesting also for the possible applications to the phenomenology. Indeed, the calculation of the $\gamma^* \rightarrow V$ impact factor is the first step towards the application of BFKL approach to the description of processes such as the vector meson electroproduction $\gamma^* p \rightarrow Vp$, being carried out at the HERA collider, and the production of two mesons in the photon collision, $\gamma^* \gamma^* \rightarrow VV$ or $\gamma^* \gamma \rightarrow VJ/\Psi$, which can be studied at high-energy e^+e^- and $e\gamma$ colliders.

In this paper we concentrate on the NLA forward amplitude for the $\gamma^* \gamma^* \rightarrow VV$ reaction (Sec. 2). Such a process has been studied in Ref. [18] in the Born (two-gluon exchange) limit for arbitrary transverse momentum and, for the forward case only, in Ref. [19] with LLA plus an estimate of NLA effects¹.

First of all, we show how the available results for the $\gamma^* \rightarrow V$ impact factor (Sec. 3) and the BFKL Green's function can be put together to build up the NLA amplitude of the $\gamma^* \gamma^* \rightarrow VV$ process in the $\overline{\text{MS}}$ scheme (Sec. 4). Then we restrict ourselves to the particular case of collision of virtual photons with equal virtualities and present some numerical estimates of our result, aimed at showing the extent of the contributions to the NLA amplitude from the impact factor and from the NLA kernel and the dependence on the energy scale introduced in the BFKL approach and on the renormalization scale which appears in the $\overline{\text{MS}}$ scheme. We show that, despite being the NLA corrections large and of opposite sign with respect to the leading order, it is possible to achieve a well-behaved form of the amplitude, by a suitable choice of the energy and renormalization scale parameters (Sec. 5).

Then, we compare different procedures to optimize the perturbative result and different representations of the amplitude, in order to have an estimate of the systematic effects which underlie our determination (Sec. 6). Finally, we calculate the differential cross section at the minimum squared momentum transfer and compare it with the approach of Ref. [19] (Sec. 7).

The use in our approach of the BFKL kernel improved by the inclusion of subleading terms generated by renormalization group analysis, which has been suggested to cure the instabilities in the behavior of the BFKL Green's function in the next-to-leading approximation [21], has been studied in Ref. [22] and is presented in Ref. [23]. The use of such an improvement has allowed for the numerical determination of the amplitude also in the case of colliding photons with strongly ordered virtuality.

¹ The QCD factorization properties of this amplitude have been studied in Ref. [20].

2. The amplitude for the electroproduction of two light vector mesons: kinematics and BFKL structure

We consider the production of two light vector mesons ($V = \rho^0, \omega, \phi$) in the collision of two virtual photons,

$$\gamma^*(p)\gamma^*(p') \rightarrow V(p_1)V(p_2). \quad (2.1)$$

Here, p_1 and p_2 are taken as Sudakov vectors satisfying $p_1^2 = p_2^2 = 0$ and $2(p_1 p_2) = s$; the virtual photon momenta are instead

$$p = \alpha p_1 - \frac{Q_1^2}{\alpha s} p_2, \quad p' = \alpha' p_2 - \frac{Q_2^2}{\alpha' s} p_1, \quad (2.2)$$

so that the photon virtualities turn to be $p^2 = -Q_1^2$ and $(p')^2 = -Q_2^2$. We consider the kinematics when

$$s \gg Q_{1,2}^2 \gg \Lambda_{\text{QCD}}^2, \quad (2.3)$$

and

$$\alpha = 1 + \frac{Q_2^2}{s} + \mathcal{O}(s^{-2}), \quad \alpha' = 1 + \frac{Q_1^2}{s} + \mathcal{O}(s^{-2}). \quad (2.4)$$

In this case vector mesons are produced by longitudinally polarized photons in the longitudinally polarized state [15]. Other helicity amplitudes are power suppressed, with a suppression factor $\sim m_V/Q_{1,2}$. We will discuss here the amplitude of the forward scattering, *i.e.* when the transverse momenta of produced V mesons are zero or when the variable $t = (p_1 - p)^2$ takes its maximal value $t_0 = -Q_1^2 Q_2^2 / s + \mathcal{O}(s^{-2})$.

The forward amplitude in the BFKL approach may be presented as follows

$$\begin{aligned} \text{Im}_s(\mathcal{A}) &= \frac{s}{(2\pi)^2} \int \frac{d^2 \vec{q}_1}{\vec{q}_1^2} \Phi_1(\vec{q}_1, s_0) \int \frac{d^2 \vec{q}_2}{\vec{q}_2^2} \Phi_2(-\vec{q}_2, s_0) \\ &\times \int_{\delta-i\infty}^{\delta+i\infty} \frac{d\omega}{2\pi i} \left(\frac{s}{s_0} \right)^\omega G_\omega(\vec{q}_1, \vec{q}_2). \end{aligned} \quad (2.5)$$

This representation for the amplitude is valid with NLA accuracy. Here $\Phi_1(\vec{q}_1, s_0)$ and $\Phi_2(-\vec{q}_2, s_0)$ are the impact factors describing the transitions $\gamma^*(p) \rightarrow V(p_1)$ and $\gamma^*(p') \rightarrow V(p_2)$, respectively. The Green's function in (2.5) obeys the BFKL equation

$$\delta^2(\vec{q}_1 - \vec{q}_2) = \omega G_\omega(\vec{q}_1, \vec{q}_2) - \int d^2 \vec{q} K(\vec{q}_1, \vec{q}) G_\omega(\vec{q}, \vec{q}_2), \quad (2.6)$$

where $K(\vec{q}_1, \vec{q}_2)$ is the BFKL kernel. The scale s_0 is artificial. It is introduced in the BFKL approach at the time to perform the Mellin transform from the s -space to the complex angular momentum plane and must disappear in the full expression for the amplitude at each fixed order of approximation. Using the result for the meson NLA impact factor such cancellation was demonstrated explicitly in Ref. [15] for the process in question.

3. The impact factor for the virtual photon to light vector meson transition

The definition of impact factor (IF) has been given in Ref. [6]; in the case of scattering of the particle A off a reggeized gluon with momentum q_1 , for transverse momentum $\vec{\Delta}$ and singlet color representation in the t -channel, the IF has the form [9]

$$\begin{aligned} \Phi_{A \rightarrow A'}(\vec{q}_1, \vec{\Delta}, s_0) &= \frac{\delta^{cc'}}{\sqrt{N_c^2 - 1}} \left[\left(\frac{s_0}{\vec{q}_1^2} \right)^{\frac{1}{2}\omega(-\vec{q}_1^2)} \left(\frac{s_0}{(\vec{q}_1 - \vec{\Delta})^2} \right)^{\frac{1}{2}\omega(-(\vec{q}_1 - \vec{\Delta})^2)} \right. \\ &\times \sum_{\{f\}} \int \frac{d\kappa}{2\pi} \theta(s_A - \kappa) d\rho_f \Gamma_{A\{f\}}^c \left(\Gamma_{A'\{f\}}^{c'} \right)^* \Big] \\ &- \frac{1}{2} \int \frac{d^{D-2}k}{\vec{k}^2(\vec{k} - \vec{\Delta})^2} \Phi_{A \rightarrow A'}^{\text{Born}}(\vec{k}, \vec{\Delta}, s_0) \mathcal{K}_r^{\text{Born}}(\vec{k}, \vec{q}_1, \vec{\Delta}) \ln \left(\frac{s_A^2}{s_0(\vec{k} - \vec{q}_1)^2} \right). \quad (3.1) \end{aligned}$$

Here $\omega(t)$ is the reggeized gluon trajectory in the LLA. The integration in the first term of Eq. (3.1) is done over the phase space $d\rho_f$ and over the squared invariant mass κ of the system $\{f\}$ produced in the fragmentation region of the particle A , $\Gamma_{A\{f\}}^c$ are the related particle–Reggeon effective vertices. The second term in Eq. (3.1) is the counterterm for the LLA part of the first one, so that the logarithmic dependence of both terms on the intermediate parameter $s_A \rightarrow \infty$ disappears in their sum. The scale s_0 is artificial and must disappear in the amplitude, to the given accuracy. The definition (3.1) guarantees the infrared finiteness of the IFs of colorless particles [24].

Here we study the NLA forward ($\vec{\Delta} = 0$) IF for the transition of a virtual photon to a light neutral meson $\Phi_{\gamma^* \rightarrow V}$, $V = \rho^0, \omega, \phi$ (see Fig. 1). We use the auxiliary Sudakov vectors p_1 and p_2 , such that $p_1^2 = p_2^2 = 0$ and $2(p_1 p_2) = s$. The virtual photon momentum is $p = p_1 - (Q^2/s)p_2$, while Reggeon momenta are:

$$\begin{aligned}
q &= \frac{\kappa + Q^2 + \vec{q}^2}{s} p_2 + q_\perp, & q^2 = q_\perp^2 = -\vec{q}^2, \\
q' &= \frac{\kappa + \vec{q}^2}{s} p_2 + q_\perp.
\end{aligned} \tag{3.2}$$

In the forward case under consideration the momentum transfer vector has only the longitudinal component, $q - q' = \zeta p_2$. Both the square of the Reggeon transverse momentum \vec{q}^2 and the virtuality of the photon Q^2 are assumed to be much larger than any hadronic scale. Thus we neglect all power suppressed contributions and, therefore, the mass of the vector meson mass is put equal to zero and its momentum is identified with the Sudakov vector p_1 .

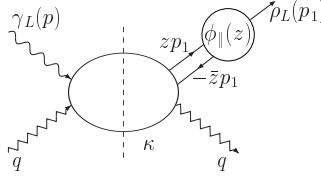


Fig. 2. The kinematics of the virtual photon to vector meson impact factor.

It is possible to show (see Ref. [15] for details) that in this kinematics the IF can be calculated in the collinear factorization framework [25–27] which was developed for the QCD description of hard exclusive processes. It turns out that the dominant helicity amplitude is a transition of the longitudinally polarized photon γ_L^* into the longitudinally polarized meson V_L , and that both in LLA and in NLA the expression for the IF factorizes into the convolution²

$$\Phi_{\gamma_L^* \rightarrow V_L}(\alpha, s_0) = -\frac{4\pi e_q f_V \delta^{cc'}}{N_c Q} \int_0^1 dz T_H(z, \alpha, s_0, \mu_F, \mu_R) \phi_{||}(z, \mu_F) \tag{3.3}$$

of a perturbatively calculable hard-scattering amplitude, T_H , and a meson twist-2 distribution amplitude, $\phi_{||}(z)$ [28]. Here $\mu_F^2 \sim Q^2, \vec{q}^2$ is a factorization scale at which soft and hard physics factorizes according to Eq. (3.3). The variable z corresponds to the longitudinal momentum fraction carried by the quark, for the antiquark the fraction is $\bar{z} = 1 - z$. Finally, we introduced the ratio $\alpha = \vec{q}^2/Q^2$. For the cases of ρ^0 , ω and ϕ meson production, e_q in Eq. (3.3) should be replaced by $e/\sqrt{2}$, $e/(3\sqrt{2})$ and $-e/3$, respectively.

² Here and in the following we consider the *color unprojected* IF.

We perform calculations with unrenormalized quantities, the bare strong coupling constant α_S and the bare meson distribution amplitude $\phi_{\parallel}^{(0)}(z)$. Therefore, the NLA expression for the hard-scattering amplitude T_H expressed in terms of these quantities contains both ultraviolet and infrared divergences, appearing as poles in the common dimensional regularization parameter ε . The ultraviolet divergences disappear after the strong coupling constant renormalization. The surviving infrared divergences are only due to collinear singularities, the soft singularities cancel as usual after summing the “virtual” and the “real” parts of the radiative corrections. Since IFs should be infrared-finite objects for physical transitions, it must be possible to absorb the remaining infrared divergences into the definition of the non-perturbative distribution amplitude. This is achieved by the substitution of the bare distribution amplitude by the renormalized one (see Ref. [15] for details).

The calculation of the lowest order contribution to the IF is straightforward (see Ref. [15]). For leading power asymptotics, the dominant contribution is given by the production of a longitudinally polarized meson. The LLA result for the hard-scattering amplitude entering the IF is

$$T_H^{(0)}(z, \alpha, s_0, \mu_F, \mu_R) = \alpha_S \frac{\alpha}{\alpha + z\bar{z}}. \quad (3.4)$$

Due to the collinear factorization, which effectively puts some fermion lines on the mass-shell, the complexity of the intermediate state contributing to the IF is reduced in comparison to the case of the virtual photon IF $\Phi_{\gamma^* \rightarrow \gamma^*}$. Actually things go as if we had one particle less in the intermediate state.

In the NLA there are two contributions to the IF, from the two-particle quark–antiquark ($q\bar{q}$) and from three-particle quark–antiquark–gluon ($q\bar{q}g$) intermediate states:

$$T_H^{(1)} = T^{(q\bar{q})} + T^{(q\bar{q}g)}. \quad (3.5)$$

To calculate the IF in the NLA one has to know the ($q\bar{q}$) production vertices with NLA accuracy and the ($q\bar{q}g$) ones at the Born level. To calculate $T^{(q\bar{q})}$ one needs to convolute the NLA photon–Reggeon vertex $\Gamma_{\gamma^* q\bar{q}}^{(1)}$ [13] with the Born Reggeon–meson vertex $\Gamma_{V_L^* q\bar{q}}^{(0)}$ [15] and the Born photon–Reggeon vertex $\Gamma_{\gamma_L^* q\bar{q}}^{(0)}$ [13, 29] with the NLA Reggeon–meson vertex $\Gamma_{V_L^* q\bar{q}}^{(1)}$ [15]. To evaluate $T^{(q\bar{q}g)}$ one needs to convolute Born photon–Reggeon vertex $\Gamma_{\gamma_L^* q\bar{q}g}^{(0)}$ [13] with the Born Reggeon–meson vertex $\Gamma_{V_L^* q\bar{q}g}^{(0)}$ [15].

Taking also into account the so-called s_A -counterterm (last term in Eq. (3.1)) and summing up all the contributions, one gets for the *renormalized* hard scattering amplitude:

$$T_H(z, \alpha, s_0, \mu_F, \mu_R)|_{\alpha \rightarrow 0} = \alpha_S(\mu_R) \frac{\alpha}{\alpha + z\bar{z}} \left\{ 1 + \frac{\alpha_S(\mu_R)}{4\pi} [\tau(z) + \tau(\bar{z})] \right\}, \quad (3.6)$$

where the expression for $\tau(z)$ is given in Ref. [15].

Using this result and the forward BFKL Green's function it is possible to build the forward amplitude of the process $\gamma_1^*(Q_1^2)\gamma_2^*(Q_2^2) \rightarrow \rho_1\rho_2$ in the NLA.

4. Building up the amplitude

It is convenient to work in the transverse momentum representation, where “transverse” is related to the plane orthogonal to the vector mesons momenta. In this representation, defined by

$$\hat{q}|\vec{q}_i\rangle = \vec{q}_i|\vec{q}_i\rangle \quad (4.1)$$

$$\langle \vec{q}_1|\vec{q}_2\rangle = \delta^{(2)}(\vec{q}_1 - \vec{q}_2), \quad \langle A|B\rangle = \langle A|\vec{k}\rangle\langle \vec{k}|B\rangle = \int d^2k A(\vec{k})B(\vec{k}), \quad (4.2)$$

the kernel of the operator \hat{K} is

$$K(\vec{q}_2, \vec{q}_1) = \langle \vec{q}_2|\hat{K}|\vec{q}_1\rangle \quad (4.3)$$

and the equation for the Green's function reads

$$\hat{1} = (\omega - \hat{K})\hat{G}_\omega \quad (4.4)$$

its solution being

$$\hat{G}_\omega = (\omega - \hat{K})^{-1}. \quad (4.5)$$

The kernel is given as an expansion in the strong coupling,

$$\hat{K} = \bar{\alpha}_s \hat{K}^0 + \bar{\alpha}_s^2 \hat{K}^1, \quad (4.6)$$

where

$$\bar{\alpha}_s = \frac{\alpha_s N_c}{\pi} \quad (4.7)$$

and N_c is the number of colors. In Eq. (4.6) \hat{K}^0 is the BFKL kernel in the LLA, \hat{K}^1 represents the NLA correction.

The impact factors are also presented as an expansion in α_s

$$\Phi_{1,2}(\vec{q}) = \alpha_s D_{1,2} \left[C_{1,2}^{(0)}(\vec{q}^2) + \bar{\alpha}_s C_{1,2}^{(1)}(\vec{q}^2) \right], \quad D_{1,2} = -\frac{4\pi e_q f_V}{N_c Q_{1,2}} \sqrt{N_c^2 - 1}, \quad (4.8)$$

where f_V is the meson dimensional coupling constant ($f_\rho \approx 200$ MeV) and e_q should be replaced by $e/\sqrt{2}$, $e/(3\sqrt{2})$ and $-e/3$ for the case of ρ^0 , ω and ϕ meson production, respectively.

In the collinear factorization approach the meson transition impact factor is given as a convolution of the hard scattering amplitude for the production of a collinear quark-antiquark pair with the meson distribution amplitude (DA). The integration variable in this convolution is the fraction z of the meson momentum carried by the quark ($\bar{z} \equiv 1 - z$ is the momentum fraction carried by the antiquark):

$$C_{1,2}^{(0)}(\vec{q}^2) = \int_0^1 dz \frac{\vec{q}^2}{\vec{q}^2 + z\bar{z}Q_{1,2}^2} \phi_{\parallel}(z). \quad (4.9)$$

The NLA correction to the hard scattering amplitude, for a photon with virtuality equal to Q^2 , is defined as follows

$$C^{(1)}(\vec{q}^2) = \frac{1}{4N_c} \int_0^1 dz \frac{\vec{q}^2}{\vec{q}^2 + z\bar{z}Q^2} [\tau(z) + \tau(1-z)] \phi_{\parallel}(z), \quad (4.10)$$

with $\tau(z)$ given in the Eq. (75) of Ref. [15]. $C_{1,2}^{(1)}(\vec{q}^2)$ are given by the previous expression with Q^2 replaced everywhere in the integrand by Q_1^2 and Q_2^2 , respectively.

The distribution amplitude may be presented as an expansion in Gegenbauer polynomials

$$\phi_{\parallel}(z, \mu_F) = 6z(1-z) \left[1 + a_2(\mu_F) C_2^{3/2}(2z-1) + a_4(\mu_F) C_4^{3/2}(2z-1) + \dots \right]. \quad (4.11)$$

The scale dependence of $a_n(\mu_F)$ is well known [25–27]:

$$a_n(\mu_F) = L^{\gamma_n/\beta_0} a_n(\mu), \quad (4.12)$$

where $L = \alpha_s(\mu_F)/\alpha_s(\mu)$ and

$$\beta_0 = \frac{11N_c}{3} - \frac{2n_f}{3} \quad (4.13)$$

is the leading coefficient of the QCD β -function, with n_f the number of active quark flavors. The anomalous dimensions γ_n are positive and grow with n . Therefore, any DA approaches the asymptotic form $\phi_{\parallel}^{\text{as}}(z) = 6z(1-z)$ at large μ_F^3 .

³ The dependence of the resulting amplitude on μ_F is subleading. Due to the collinear counterterm, see Eq. (72) of [15], the NLA correction to the meson impact factor contains a term proportional to $\ln(\mu_F)$, see Eq. (75) of [15], which compensates in the amplitude with NLA accuracy the effect of the meson DA variation with μ_F .

Below we will use the DA in the asymptotic form. Besides the simplicity of the following presentation, the reason is twofold. Presumably, the form of DA chosen at low μ_F will affect mainly only the overall normalization of the amplitude but not the sum of BFKL energy logarithms and the resulting dependence of the amplitude on the energy in which we are primarily interested in this study. Another point is that, according to QCD sum rules estimates [28], $a_2(1 \text{ GeV})$ is 0.18 ± 0.10 for ρ and 0 ± 0.1 for ϕ . Therefore, $\phi_{\parallel}^{\text{as}}$ may be indeed a good approximation for the DA of light vector mesons. Integrating over z in (4.9) with $\phi_{\parallel}(z, \mu_F^2) = \phi_{\parallel}^{\text{as}}(z)$, we obtain, for photon virtuality Q^2 ,

$$C^{(0)} \left(\alpha = \frac{\vec{q}^2}{Q^2} \right) = 6\alpha \left[1 - \frac{\alpha}{c} \ln \frac{2c+1}{2c-1} \right], \quad (4.14)$$

where $c = \sqrt{\alpha + 1/4}$. $C_{1,2}^{(0)}$ are given by the previous expression with Q^2 replaced by Q_1^2 and Q_2^2 , respectively. For the NLA term $C_{1,2}^{(1)}(\vec{q}^2)$ the integration over z can be performed by a numerical calculation.

To determine the amplitude with NLA accuracy we need an approximate solution of Eq. (4.5). With the required accuracy this solution is

$$\hat{G}_{\omega} = (\omega - \bar{\alpha}_s \hat{K}^0)^{-1} + (\omega - \bar{\alpha}_s \hat{K}^0)^{-1} \left(\bar{\alpha}_s^2 \hat{K}^1 \right) (\omega - \bar{\alpha}_s \hat{K}^0)^{-1} + \mathcal{O} \left[\left(\bar{\alpha}_s^2 \hat{K}^1 \right)^2 \right]. \quad (4.15)$$

The basis of eigenfunctions of the LLA kernel,

$$\hat{K}^0 |\nu\rangle = \chi(\nu) |\nu\rangle, \quad \chi(\nu) = 2\psi(1) - \psi\left(\frac{1}{2} + i\nu\right) - \psi\left(\frac{1}{2} - i\nu\right), \quad (4.16)$$

is given by the following set of functions:

$$\langle \vec{q} | \nu \rangle = \frac{1}{\pi\sqrt{2}} (\vec{q}^2)^{i\nu - \frac{1}{2}}, \quad (4.17)$$

for which the orthonormality condition takes the form

$$\langle \nu' | \nu \rangle = \int \frac{d^2 \vec{q}}{2\pi^2} (\vec{q}^2)^{i\nu - i\nu' - 1} = \delta(\nu - \nu'). \quad (4.18)$$

The action of the full NLA BFKL kernel on these functions may be expressed as follows:

$$\begin{aligned} \hat{K} |\nu\rangle &= \bar{\alpha}_s(\mu_R) \chi(\nu) |\nu\rangle + \bar{\alpha}_s^2(\mu_R) \left(\chi^{(1)}(\nu) + \frac{\beta_0}{4N_c} \chi(\nu) \ln(\mu_R^2) \right) |\nu\rangle \\ &+ \bar{\alpha}_s^2(\mu_R) \frac{\beta_0}{4N_c} \chi(\nu) \left(i \frac{\partial}{\partial \nu} \right) |\nu\rangle, \end{aligned} \quad (4.19)$$

where the first term represents the action of LLA kernel, while the second and the third ones stand for the diagonal and the non-diagonal parts of the NLA kernel. The function $\chi^{(1)}(\nu)$, calculated in Ref. [2], is conveniently represented in the form

$$\chi^{(1)}(\nu) = -\frac{\beta_0}{8N_c} \left(\chi^2(\nu) - \frac{10}{3}\chi(\nu) - i\chi'(\nu) \right) + \bar{\chi}(\nu), \quad (4.20)$$

where

$$\begin{aligned} \bar{\chi}(\nu) = & -\frac{1}{4} \left[\frac{\pi^2 - 4}{3} \chi(\nu) - 6\zeta(3) - \chi''(\nu) - \frac{\pi^3}{\cosh(\pi\nu)} \right. \\ & \left. + \frac{\pi^2 \sinh(\pi\nu)}{2\nu \cosh^2(\pi\nu)} \left(3 + \left(1 + \frac{n_f}{N_c^3} \right) \frac{11 + 12\nu^2}{16(1 + \nu^2)} \right) + 4\phi(\nu) \right], \end{aligned} \quad (4.21)$$

$$\phi(\nu) = 2 \int_0^1 dx \frac{\cos(\nu \ln(x))}{(1+x)\sqrt{x}} \left[\frac{\pi^2}{6} - \text{Li}_2(x) \right],$$

$$\text{Li}_2(x) = - \int_0^x dt \frac{\ln(1-t)}{t}. \quad (4.22)$$

Here and below $\chi'(\nu) = d(\chi(\nu))/d\nu$ and $\chi''(\nu) = d^2(\chi(\nu))/d^2\nu$.

We will need also the $|\nu\rangle$ representation for the impact factors, which is defined by the following expressions

$$\frac{C_1^{(0)}(\vec{q}^2)}{\vec{q}^2} = \int_{-\infty}^{+\infty} d\nu' c_1(\nu') \langle \nu' | \vec{q} \rangle, \quad \frac{C_2^{(0)}(\vec{q}^2)}{\vec{q}^2} = \int_{-\infty}^{+\infty} d\nu c_2(\nu) \langle \vec{q} | \nu \rangle, \quad (4.23)$$

$$\begin{aligned} c_1(\nu) &= \int d^2\vec{q} C_1^{(0)}(\vec{q}^2) \frac{(\vec{q}^2)^{i\nu - \frac{3}{2}}}{\pi\sqrt{2}}, \\ c_2(\nu) &= \int d^2\vec{q} C_2^{(0)}(\vec{q}^2) \frac{(\vec{q}^2)^{-i\nu - \frac{3}{2}}}{\pi\sqrt{2}}, \end{aligned} \quad (4.24)$$

and by similar equations for $c_1^{(1)}(\nu)$ and $c_2^{(1)}(\nu)$ from the NLA corrections to the impact factors, $C_1^{(1)}(\vec{q}^2)$ and $C_2^{(1)}(\vec{q}^2)$.

Using (4.15) and (4.19) one can derive, after some algebra, the following representation for the amplitude:

$$\begin{aligned}
\frac{\text{Im}_s(\mathcal{A})}{D_1 D_2} &= \frac{s}{(2\pi)^2} \int_{-\infty}^{+\infty} d\nu \left(\frac{s}{s_0} \right)^{\bar{\alpha}_s(\mu_R) \chi(\nu)} \alpha_s^2(\mu_R) c_1(\nu) c_2(\nu) \\
&\times \left[1 + \bar{\alpha}_s(\mu_R) \left(\frac{c_1^{(1)}(\nu)}{c_1(\nu)} + \frac{c_2^{(1)}(\nu)}{c_2(\nu)} \right) + \bar{\alpha}_s^2(\mu_R) \ln \left(\frac{s}{s_0} \right) \right. \\
&\times \left. \left(\bar{\chi}(\nu) + \frac{\beta_0}{8N_c} \chi(\nu) \left[-\chi(\nu) + \frac{10}{3} + i \frac{d \ln(\frac{c_1(\nu)}{c_2(\nu)})}{d\nu} + 2 \ln(\mu_R^2) \right] \right) \right]. \quad (4.25)
\end{aligned}$$

We find that

$$c_{1,2}(\nu) = \frac{(Q_{1,2}^2)^{\pm i\nu - \frac{1}{2}}}{\sqrt{2}} \frac{\Gamma^2[\frac{3}{2} \pm i\nu]}{\Gamma[3 \pm 2i\nu]} \frac{6\pi}{\cosh(\pi\nu)}, \quad (4.26)$$

$$c_1(\nu) c_2(\nu) = \frac{1}{Q_1 Q_2} \left(\frac{Q_1^2}{Q_2^2} \right)^{i\nu} \frac{9\pi^3(1+4\nu^2) \sinh(\pi\nu)}{32\nu(1+\nu^2) \cosh^3(\pi\nu)}, \quad (4.27)$$

$$\begin{aligned}
i \frac{d \ln(\frac{c_1(\nu)}{c_2(\nu)})}{d\nu} &= 2 \left[\psi(3+2i\nu) + \psi(3-2i\nu) - \psi\left(\frac{3}{2} + i\nu\right) \right. \\
&\quad \left. - \psi\left(\frac{3}{2} - i\nu\right) - \ln(Q_1 Q_2) \right]. \quad (4.28)
\end{aligned}$$

It can be useful to separate from the NLA correction to the impact factor the terms containing the dependence on s_0 and on β_0 ,

$$\begin{aligned}
C^{(1)}(\vec{q}^2) &= \int_0^1 dz \frac{\vec{q}^2}{\vec{q}^2 + z\bar{z}Q^2} \phi_{\parallel}(z) \left[\frac{1}{4} \ln \left(\frac{s_0}{Q^2} \right) \ln \left(\frac{(\alpha + z\bar{z})^4}{\alpha^2 z^2 \bar{z}^2} \right) \right. \\
&\quad \left. + \frac{\beta_0}{4N_c} \left(\ln \left(\frac{\mu_R^2}{Q^2} \right) + \frac{5}{3} - \ln(\alpha) \right) + \dots \right]. \quad (4.29)
\end{aligned}$$

Accordingly, one can write

$$c_{1,2}^{(1)}(\nu) = \tilde{c}_{1,2}^{(1)}(\nu) + \bar{c}_{1,2}^{(1)}(\nu), \quad (4.30)$$

where $\tilde{c}_{1,2}^{(1)}(\nu)$ are the contributions from the terms isolated in the previous equation and $\bar{c}_{1,2}^{(1)}(\nu)$ represent the rest. After straightforward calculations we found that:

$$\begin{aligned} \frac{\tilde{c}_1^{(1)}(\nu)}{c_1(\nu)} + \frac{\tilde{c}_2^{(1)}(\nu)}{c_2(\nu)} = \ln\left(\frac{s_0}{Q_1 Q_2}\right) \chi(\nu) + \frac{\beta_0}{2N_c} \left[\ln\left(\frac{\mu_R^2}{Q_1 Q_2}\right) + \frac{5}{3} + \psi(3 + 2i\nu) \right. \\ \left. + \psi(3 - 2i\nu) - \psi\left(\frac{3}{2} + i\nu\right) - \psi\left(\frac{3}{2} - i\nu\right) \right]. \quad (4.31) \end{aligned}$$

Using Eq. (4.25) we construct the following representation for the amplitude

$$\begin{aligned} \frac{Q_1 Q_2}{D_1 D_2} \frac{\text{Im}_s \mathcal{A}}{s} = \frac{1}{(2\pi)^2} \alpha_s(\mu_R)^2 \\ \times \left[b_0 + \sum_{n=1}^{\infty} \bar{\alpha}_s(\mu_R)^n b_n \left(\ln\left(\frac{s}{s_0}\right)^n + d_n(s_0, \mu_R) \ln\left(\frac{s}{s_0}\right)^{n-1} \right) \right], \quad (4.32) \end{aligned}$$

where the coefficients

$$\frac{b_n}{Q_1 Q_2} = \int_{-\infty}^{+\infty} d\nu \, c_1(\nu) c_2(\nu) \frac{\chi^n(\nu)}{n!}, \quad (4.33)$$

are determined by the kernel and the impact factors in LLA. Note that

$$b_0 = \frac{9\pi}{4} (7\zeta(3) - 6), \quad (4.34)$$

therefore, in the Born (the two-gluon exchange) limit our result coincides with that of Ref. [18].

The coefficients

$$\begin{aligned} d_n = n \ln\left(\frac{s_0}{Q_1 Q_2}\right) + \frac{\beta_0}{4N_c} \left((n+1) \frac{b_{n-1}}{b_n} \ln\left(\frac{\mu_R^2}{Q_1 Q_2}\right) - \frac{n(n-1)}{2} \right. \\ \left. + \frac{Q_1 Q_2}{b_n} \int_{-\infty}^{+\infty} d\nu \, (n+1) f(\nu) c_1(\nu) c_2(\nu) \frac{\chi^{n-1}(\nu)}{(n-1)!} \right) \\ \left. + \frac{Q_1 Q_2}{b_n} \left(\int_{-\infty}^{+\infty} d\nu \, c_1(\nu) c_2(\nu) \frac{\chi^{n-1}(\nu)}{(n-1)!} \left[\frac{\tilde{c}_1^{(1)}(\nu)}{c_1(\nu)} + \frac{\tilde{c}_2^{(1)}(\nu)}{c_2(\nu)} + (n-1) \frac{\bar{\chi}(\nu)}{\chi(\nu)} \right] \right) \right) \quad (4.35) \end{aligned}$$

are determined by the NLA corrections to the kernel and to the impact factors. Here we use the notation

$$f(\nu) = \frac{5}{3} + \psi(3 + 2i\nu) + \psi(3 - 2i\nu) - \psi\left(\frac{3}{2} + i\nu\right) - \psi\left(\frac{3}{2} - i\nu\right). \quad (4.36)$$

One should stress that both representations of the amplitude (4.32) and (4.25) are equivalent with NLA accuracy, since they differ only by next-to-NLA (NNLA) terms. Actually there exist infinitely many possibilities to write a NLA amplitude. For instance, another possibility could be to exponentiate the bulk of the kernel NLA corrections

$$\begin{aligned} \frac{\text{Im}_s(\mathcal{A})}{D_1 D_2} &= \frac{s}{(2\pi)^2} \int_{-\infty}^{+\infty} d\nu \left(\frac{s}{s_0} \right)^{\bar{\alpha}_s(\mu_R)\chi(\nu) + \bar{\alpha}_s^2(\mu_R) \left(\bar{\chi}(\nu) + \frac{\beta_0}{8N_c} \chi(\nu) \left[-\chi(\nu) + \frac{10}{3} \right] \right)} \\ &\times \alpha_s^2(\mu_R) c_1(\nu) c_2(\nu) \left[1 + \bar{\alpha}_s(\mu_R) \left(\frac{c_1^{(1)}(\nu)}{c_1(\nu)} + \frac{c_2^{(1)}(\nu)}{c_2(\nu)} \right) \right. \\ &\left. + \bar{\alpha}_s^2(\mu_R) \ln \left(\frac{s}{s_0} \right) \frac{\beta_0}{8N_c} \chi(\nu) \left(i \frac{d \ln \left(\frac{c_1(\nu)}{c_2(\nu)} \right)}{d\nu} + 2 \ln(\mu_R^2) \right) \right]. \quad (4.37) \end{aligned}$$

This form of the NLA amplitude was used in Ref. [30] (see also [31]), without account of the last two terms in the second line of (4.37), for the analysis of the total $\gamma^* \gamma^*$ cross section.

Since as we will shortly see the NLA corrections are very large, the choice of the representation for the NLA amplitude becomes practically important. In the present situation, when an approach to the calculation of the NNLA corrections is not developed yet, the series representation (4.32) is, in our opinion, a natural choice. It includes in some sense the minimal amount of NNLA contributions; moreover, its form is the closest one to the initial goal of the BFKL approach, *i.e.* to sum selected contributions in the perturbative series.

It is easily seen from Eqs. (4.32)–(4.36) that the amplitude is independent in the NLA from the choice of energy and strong coupling scales. Indeed, with the required accuracy,

$$\bar{\alpha}_s(\mu_R) = \bar{\alpha}_s(\mu_0) \left(1 - \frac{\bar{\alpha}_s(\mu_0) \beta_0}{4N_c} \ln \left(\frac{\mu_R^2}{\mu_0^2} \right) \right) \quad (4.38)$$

and therefore terms $\bar{\alpha}_s^n \ln^{n-1} s \ln s_0$ and $\bar{\alpha}_s^n \ln^{n-1} s \ln \mu_R$ cancel in (4.32).

One can trace the contributions to each d_n coefficient coming from the NLA corrections to the BFKL kernel and from the NLA impact factors:

$$d_n = d_n^{\text{ker}} + d_n^{\text{IF}}, \quad (4.39)$$

$$\begin{aligned}
d_n^{\text{IF}} = & n \ln \left(\frac{s_0}{Q_1 Q_2} \right) + \frac{\beta_0}{4N_c} \\
& \times 2 \left(\frac{b_{n-1}}{b_n} \ln \left(\frac{\mu_R^2}{Q_1 Q_2} \right) + \frac{Q_1 Q_2}{b_n} \int_{-\infty}^{+\infty} d\nu f(\nu) c_1(\nu) c_2(\nu) \frac{\chi^{n-1}(\nu)}{(n-1)!} \right) \\
& + \frac{Q_1 Q_2}{b_n} \left(\int_{-\infty}^{+\infty} d\nu c_1(\nu) c_2(\nu) \frac{\chi^{n-1}(\nu)}{(n-1)!} \left[\frac{\bar{c}_1^{(1)}(\nu)}{c_1(\nu)} + \frac{\bar{c}_2^{(1)}(\nu)}{c_2(\nu)} \right] \right). \quad (4.40)
\end{aligned}$$

The first coefficient, d_1 , is entirely due to the NLA corrections to the impact factors,

$$d_1 = d_1^{\text{IF}}, \quad d_1^{\text{ker}} = 0. \quad (4.41)$$

Let us note that in the BFKL formalism the NLA contribution to the impact factors guarantees not only independence of the amplitude from the energy scale, s_0 , but it also contains a term proportional to $\ln \mu_R$ which is important for the renorm-invariance of the predicted results, *i.e.* the dependence of the amplitude on μ_R and s_0 is subleading to the NLA accuracy.

5. Numerical results

In this Section we present some numerical results for the amplitude given in Eq. (4.32) for the $Q_1 = Q_2 \equiv Q$ kinematics, *i.e.* in the “pure” BFKL regime. The other interesting regime, $Q_1 \gg Q_2$ or *vice-versa*, where collinear effects could come heavily into the game, will not be considered here. We will emphasize in particular the dependence on the renormalization scale μ_R and s_0 in the NLA result.

In all the forthcoming figures the quantity on the vertical axis is the left-hand side of Eq. (4.32), $\text{Im}_s(\mathcal{A})Q^2/(s D_1 D_2)$. In the numerical analysis presented below we truncate the series in the right-hand side of Eq. (4.32) to $n = 20$, after having verified that this procedure gives a very good approximation of the infinite sum for the Y values $Y \leq 10$. We use the two-loop running coupling corresponding to the value $\alpha_s(M_Z) = 0.12$.

We have calculated numerically the b_n and d_n coefficients for $n_f = 5$ and $s_0 = Q^2 = \mu_R^2$, getting

$$\begin{aligned}
b_0 &= 17.0664 \\
b_1 &= 34.5920 & b_2 &= 40.7609 & b_3 &= 33.0618 & b_4 &= 20.7467 \\
b_5 &= 10.5698 & b_6 &= 4.54792 & b_7 &= 1.69128 & b_8 &= 0.554475 \\
d_1 &= -3.71087 & d_2 &= -11.3057 & d_3 &= -23.3879 & d_4 &= -39.1123 \\
d_5 &= -59.207 & d_6 &= -83.0365 & d_7 &= -111.151 & d_8 &= -143.06.
\end{aligned} \quad (5.1)$$

In this case contributions to the d_n coefficients originating from the NLA corrections to the impact factors are

$$\begin{aligned} d_1^{\text{IF}} &= -3.71087, & d_2^{\text{IF}} &= -8.4361, & d_3^{\text{IF}} &= -13.1984, & d_4^{\text{IF}} &= -18.0971, \\ d_5^{\text{IF}} &= -23.0235, & d_6^{\text{IF}} &= -27.9877, & d_7^{\text{IF}} &= -32.9676, & d_8^{\text{IF}} &= -37.9618. \end{aligned} \quad (5.2)$$

Thus, comparing (5.1) and (5.2), we see that the contribution from the kernel starts to be larger than the impact factor one only for $n \geq 4$.

These numbers make visible the effect of the NLA corrections: the d_n coefficients are negative and increasingly large in absolute values as the perturbative order increases. The NLA corrections turn to be very large. In this situation the optimization of perturbative expansion, in our case the choice of the renormalization scale μ_R and of the energy scale s_0 , becomes an important issue. Below we will adopt the principle of minimal sensitivity (PMS) [32]. Usually PMS is used to fix the value of the renormalization scale for the strong coupling. We suggest to use this principle in a broader sense, requiring in our case the minimal sensitivity of the predictions to the change of both the renormalization and the energy scales, μ_R and s_0 .

Since the dependence of results on s_0 is a feature typical of the BFKL approach and is somewhat new for the application of PMS, we will first illustrate the success of PMS in this respect on the following QED result known since a long time. In 1937 Racah calculated the total cross section for the production of e^+e^- pairs in the collisions of two heavy ions at high energies [33],

$$\sigma = \frac{28\alpha_{\text{EM}}^4 Z_1^2 Z_2^2}{27\pi m_e^2} (l^3 + Al^2 + Bl + C) + \mathcal{O}\left(\frac{1}{(p_1 p_2)}\right), \quad (5.3)$$

here $Z_{1,2}$ are the ions charges, m_e is electron mass, the ions' four-momenta are $p_{1,2}$,

$$l = \ln \frac{2(p_1 p_2)}{m_1 m_2}, \quad (5.4)$$

is the energy logarithm and $m_{1,2}$ are the masses of the ions. The contributions suppressed by the power of energy are denoted as $\mathcal{O}(1/(p_1 p_2))$.

The coefficients in front of the subleading logarithms are large and have alternating signs

$$\begin{aligned} A &= -178/28 = -6.35714, \\ B &= \frac{1}{28}(7\pi^2 + 370) = 15.6817, \\ C &= -\frac{1}{28}\left(348 + \frac{13}{2}\pi^2 - 21\zeta(3)\right) = -13.8182. \end{aligned} \quad (5.5)$$

To illustrate the application of PMS, imagine that we know only the coefficient A in front of the first subleading logarithm. Then using this knowledge we can construct the following approximation

$$\sigma^{\text{app}} = \sigma_0 \left((l-l_0)^3 + (A+3l_0)(l-l_0)^2 \right), \quad \sigma_0 = \frac{28\alpha_{\text{EM}}^4 Z_1^2 Z_2^2}{27\pi m_e^2}, \quad (5.6)$$

(an analog of NLA in the BFKL approach) where we shift the energy scale introducing the parameter l_0 . Note that the dependence of the cross section on l_0 is subleading in the approximation used in Eq. (5.6). We fix l_0 by requiring the minimal sensitivity of (5.6) to the change of this parameter. It is not difficult to find that this procedure gives $l_0 = -A/3 = 2.11905^4$. In Fig. 3 we present three curves for σ/σ_0 as a function of the energy logarithm l ; the first one was calculated using the exact result of Racah (with all subleading logarithms), the other two curves were calculated using (5.6) with $l_0 = 0$ and with the PMS value $l_0 = 2.11905$.

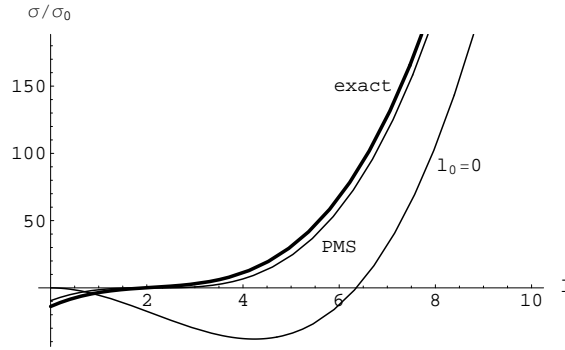


Fig. 3. σ/σ_0 as a function of the energy logarithm l for the cases of exact result of Racah, approximated result with $l_0 = -A/3$ (PMS optimal choice) and $l_0 = 0$ (kinematical scale for energy logarithms).

We see that the PMS approach gives a very good approximation to the Racah result⁵. On the other hand the procedure with $l_0 = 0$, which means that a kinematical scale for energy logarithms is used in the approximate formula, makes an awfully bad job for the whole l range presented in the figure.

⁴ Note that in this example PMS gives the value of the parameter l_0 for which the correction to the lowest approximation, $(l-l_0)^3$, vanishes. Therefore, in this case PMS gives a result which coincides with the one given by another alternative approach to optimize the approximation, the fast apparent convergence prescription [34].

⁵ The negative cross section at $l < 2$ is due to the fact that terms subleading in energy, $\mathcal{O}(1/(p_1 p_2))$ in (5.3), are not taken into account.

Returning to our problem, we apply PMS to our case requiring the minimal sensitivity of the amplitude (4.32) to the variation of μ_R and s_0 . More precisely, we replace in (4.32) $\ln(s/s_0)$ with $Y - Y_0$, where $Y = \ln(s/Q^2)$ and $Y_0 = \ln(s_0/Q^2)$, and study the dependence of the amplitude on Y_0 .

The next two figures illustrate the dependence on these parameters for $Q^2 = 24 \text{ GeV}^2$ and $n_f = 5$. In Fig. 4 (left) we show the dependence of amplitude on Y_0 for $\mu_R = 10Q$, when Y takes the values 10, 8, 6, 4, 3.

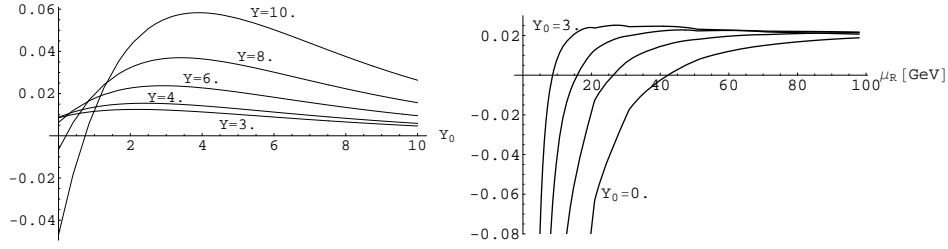


Fig. 4. Left: $\text{Im}_s(\mathcal{A})Q^2/(s D_1 D_2)$ as a function of Y_0 at $\mu_R = 10Q$. The different curves are for Y values of 10, 8, 6, 4 and 3. The photon virtuality Q^2 has been fixed to 24 GeV^2 ($n_f = 5$). Right: $\text{Im}_s(\mathcal{A})Q^2/(s D_1 D_2)$ as a function of μ_R at $Y = 6$. The different curves are, from above to below, for Y_0 values of 3, 2, 1 and 0. The photon virtuality Q^2 has been fixed to 24 GeV^2 ($n_f = 5$).

We see that for each Y the amplitude has an extremum in Y_0 near which it is not sensitive to the variation of Y_0 , or s_0 . Our choice of μ_R for this figure is motivated by the study of μ_R dependence. In Fig. 4 (right) we present the μ_R dependence for $Y = 6$; the curves from above to below are for $Y_0 = 3, 2, 1, 0$.

Varying μ_R and Y_0 we found for each Y quite large regions in μ_R and Y_0 where the amplitude is practically independent on μ_R and Y_0 . We use this value as the NLA result for the amplitude at given Y . In Fig. 5 we present the amplitude found in this way as a function of Y . The resulting curve is compared with the curve obtained from the LLA prediction when the scales are chosen as $\mu_R = 10Q$ and $Y_0 = 2.2$, in order to make the LLA curve the closest possible (of course it is not an exact statement) to the NLA one in the given interval of Y . The two horizontal lines in Fig. 5 are the Born (two-gluon exchange) predictions calculated for $\mu_R = Q$ and $\mu_R = 10Q$.

Similar procedure was applied to a lower value of the photon virtuality, $Q^2 = 5 \text{ GeV}^2$ and $n_f = 4$ (see Ref. [16] for details).

We stress that one should take with care BFKL predictions for small values of Y , since in this region the contributions suppressed by powers of the energy should be taken into account. At the lowest order in α_s such contributions are given by diagrams with quark exchange in the t -channel and are proportional in our case to $\alpha_{\text{EM}}\alpha_s f_V^2/Q^2$. At higher orders power suppressed

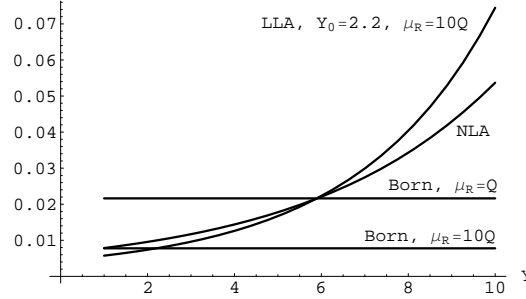


Fig. 5. $\text{Im}_s(\mathcal{A})Q^2/(s D_1 D_2)$ as a function of Y for optimal choice of the energy parameters Y_0 and μ_R (curve labeled by “NLA”). The other curves represent the LLA result for $Y_0 = 2.2$ and $\mu_R = 10Q$ and the Born (two-gluon exchange) limit for $\mu_R = Q$ and $\mu_R = 10Q$. The photon virtuality Q^2 has been fixed to 24 GeV^2 ($n_f = 5$).

contributions contain double logarithms, terms $\sim \alpha_s^n \ln^{2n} s$, which can lead to a significant enhancement. Such contributions were recently studied for the total cross section of $\gamma^* \gamma^*$ interactions [35].

If the NLA (and LLA) curves in Fig. 5 are compared with the Born (two-gluon exchange) results, one can conclude that the summation of BFKL series gives negative contribution to the Born result for $Y < 6$ if one chooses for the scale of the strong coupling in the Born amplitude the value given by the kinematics, $\mu_R = Q$. We believe that our calculations show that one should at least accept with some caution the results obtained in the Born approximation, since they do not give necessarily an estimate of the observable from below.

Another important lesson from our calculation is the very large scale for α_s (and therefore the small α_s itself) we obtain using PMS. It appears to be much bigger than the kinematical scale and looks unnatural since there is no other scale for transverse momenta in the problem at question except Q . Moreover, one can guess that at higher orders the typical transverse momenta are even smaller than Q since they “are shared” in the many-loop integrals and the strong coupling grows in the infrared. In our opinion the large values of μ_R we found is not an indication of the appearance of a new scale, but is rather a manifestation of the nature of the BFKL series. The fact is that NLA corrections are large and then, necessarily, since the exact amplitude should be renorm- and energy scale invariant, the NNLA terms should be large and of the opposite sign with respect to the NLA. We guess that if the NNLA corrections were known and we would apply PMS to the amplitude constructed as LLA + NLA-corrections + NNLA-corrections, we would obtain in such calculation more natural values of μ_R .

In the last years strong efforts have been devoted to the improvement of the NLA BFKL kernel as a consequence of the analysis of collinear singularities of the NLA corrections and by the account of further collinear terms beyond NLA [21, 36]. This strategy has something in common with ours, in the sense that it is also inspired by renormalization-group invariance and it also leads to the addition of terms beyond the NLA. These extra-terms are large and of opposite sign with respect to the NLA contribution, so that they partially compensate the NLA corrections. The findings of the present work suggest, however, that the corrections to the impact factors heavily contribute to the NLA amplitude, being even dominating in some interval of non-asymptotically high energies. Moreover, by inspection of the structure of the amplitude in the regime of strongly asymmetric photon virtualities, one can deduce that also the impact factors generate collinear terms which add up to those arising from the kernel, see *e.g.* Eqs. (84) and (85) of Ref. [15]. This leads us to the conclusion that in the approaches based on kernel improvement the additional information coming from impact factors should somehow be taken into account when available. These issues certainly deserve further investigation and we believe that useful hints in this direction can be gained from the study of the $\gamma^*\gamma^* \rightarrow VV$ amplitude in the regime of strongly ordered photon virtualities [22, 23].

We conclude this section with a comment on the possible implications of our results for mesons electroproduction to the phenomenologically more important case of the $\gamma^*\gamma^*$ total cross section. By numerical inspection we have found that the ratios b_n/b_0 we got for the meson case agree for $n = 1 \div 10$ at $1 \div 2\%$ accuracy level with the analogous ratios for the longitudinal photon case and at $3.5 \div 30\%$ accuracy level with those for the transverse photon case. Should this similar behavior persist also in the NLA, our predictions could be easily translated to estimates of the $\gamma^*\gamma^*$ total cross section.

6. Study of systematic effects

It is important to have an estimate of the systematic uncertainty which plagues our determination of the energy behavior of the amplitude. The main sources of systematic effects are given by the choice of the representation of the amplitude and by the optimization method adopted. In the following, we compare the determination of the amplitude at $Q^2 = 24 \text{ GeV}^2$ ($n_f = 5$) through the PMS method, given in Fig. 5, with other determinations obtained changing either the representation of the amplitude or the optimization method.

At first, we compare the series and the “exponentiated” determinations using in both case the PMS method. The procedure we followed to determine the energy behavior of the “exponentiated” amplitude is straightforward: for

each fixed value of Y we determined the optimal choice of the parameters μ_R and Y_0 for which the amplitude given in Eq. (4.37) is the least sensitive to their variation. Also in this case we could see wide regions of stability of the amplitude in the (μ_R, Y_0) plane. The optimal values of μ_R and Y_0 are quite similar to those obtained in the case of the series representation, with only a slight decrease of the optimal μ_R . In Fig. 6 (left) we show the result and compare it to the PMS determination from the series representation. The two curves are in good agreement at the lower energies, the deviation increasing for large values of Y . It should be stressed, however, that the applicability domain of the BFKL approach is determined by the condition $\bar{\alpha}_s(\mu_R)Y \sim 1$ and, for $Q^2 = 24 \text{ GeV}^2$ and for the typical optimal values of μ_R , one gets from this condition $Y \sim 5$. Around this value the discrepancy between the two determinations is within a few percent.

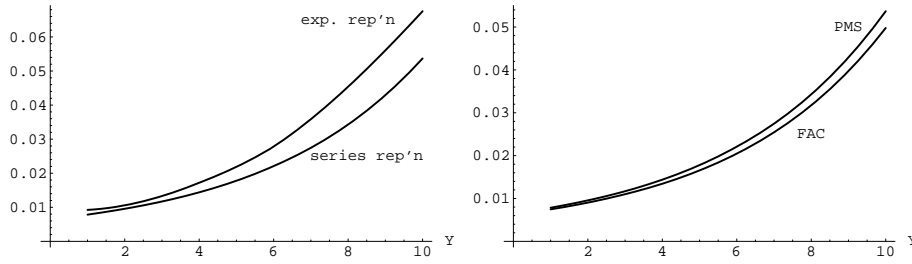


Fig. 6. Left: $\text{Im}_s(\mathcal{A})Q^2/(s D_1 D_2)$ as a function of Y at $Q^2=24 \text{ GeV}^2$ ($n_f = 5$) from series and “exponentiated” representations, in both cases with the PMS optimization method. Right: $\text{Im}_s(\mathcal{A}_{\text{series}})Q^2/(s D_1 D_2)$ as a function of Y at $Q^2=24 \text{ GeV}^2$ ($n_f = 5$) from the series representation with PMS and FAC optimization methods.

As a second check, we changed the optimization method and applied it both to the series and to the “exponentiated” representation. The method considered is the fast apparent convergence (FAC) method [34], whose strategy, when applied to a usual perturbative expansion, is to fix the renormalization scale to the value for which the highest order correction term is exactly zero. In our case, the application of the FAC method requires an adaptation, for two reasons: the first is that we have two energy parameters in the game, μ_R and Y_0 , the second is that, if only strict NLA corrections are taken, the amplitude does not depend at all on these parameters.

Therefore, in the case of the series representation, Eq. (4.32), we choose to put to zero the sum

$$\frac{1}{(2\pi)^2} \alpha_s(\mu_R)^2 \sum_{n=1}^{\infty} \bar{\alpha}_s(\mu_R)^n b_n d_n(s_0, \mu_R) \ln \left(\frac{s}{s_0} \right)^{n-1}$$

and found for each fixed Y the values of μ_R and Y_0 for which the vanishing occurs. This gives a line of values in the (μ_R, Y_0) plane, among which the optimal choice is done applying a minimum sensitivity criterion. The result is shown in Fig. 6 (right). The agreement with the series representation with the PMS method is rather good over a wide energy range.

In the case of the “exponentiated” amplitude”, Eq. (4.37), we proceeded in the same way, but requiring the vanishing of the expression given by the right-hand side of Eq. (4.37) minus the LLA amplitude, *i.e.*

$$\frac{\text{Im}_s(\mathcal{A}_{\text{exp}})}{D_1 D_2} - \frac{s}{(2\pi)^2} \int_{-\infty}^{+\infty} d\nu \left(\frac{s}{s_0} \right)^{\bar{\alpha}_s(\mu_R)\chi(\nu)} \alpha_s^2(\mu_R) c_1(\nu) c_2(\nu).$$

In Fig. 7 (left) the result is compared with series representation in the PMS method: there is nice agreement over the whole energy range considered.

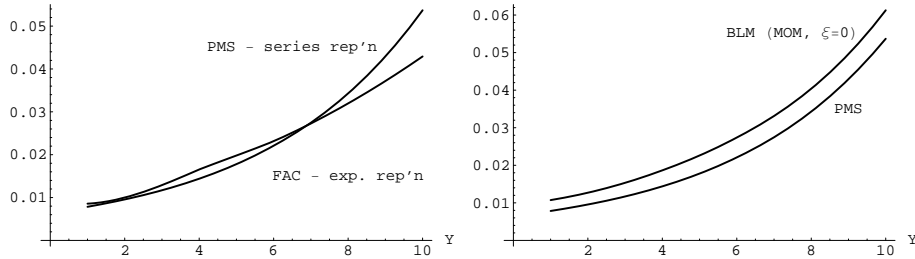


Fig. 7. Left: $\text{Im}_s(\mathcal{A})Q^2/(s D_1 D_2)$ as a function of Y at $Q^2 = 24 \text{ GeV}^2$ ($n_f = 5$) from the series representation with the PMS optimization method and from the “exponentiated” representation with the FAC optimization method. Right: $\text{Im}_s(\mathcal{A})Q^2/(s D_1 D_2)$ as a function of Y at $Q^2 = 24 \text{ GeV}^2$ ($n_f = 5$) from the series representation with PMS and BLM optimization methods.

Another popular optimization procedure is the Brodsky–Lepage–MacKenzie (BLM) method [37], which amounts to perform a finite renormalization to a physical scheme and then choose the renormalization scale in order to remove the β_0 -dependent part. We applied this method only to the series representation, Eq. (4.32), and proceeded as follows: we first performed a finite renormalization to the momentum (MOM) scheme with $\xi = 0$ (see Ref. [30]),

$$\alpha_s \rightarrow \alpha_s \left[1 + T_{\text{MOM}}(\xi = 0) \frac{\alpha_s}{\pi} \right], \quad T_{\text{MOM}}(\xi = 0) = T_{\text{MOM}}^{\text{conf}} + T_{\text{MOM}}^{\beta},$$

$$T_{\text{MOM}}^{\text{conf}} = \frac{N_c}{8} \frac{17}{2} I, \quad T_{\text{MOM}}^{\beta} = -\frac{\beta_0}{2} \left[1 + \frac{2}{3} I \right], \quad I \simeq 2.3439,$$

then, we chose Y_0 and μ_R in order to make the term proportional to β_0 in the resulting amplitude vanish. We observe that the β_0 -dependence in the series representation of the amplitude is hidden into the d_n coefficients, Eq. (4.35). Among the resulting pairs of values for Y_0 and μ_R , we determined the optimal one according to minimum sensitivity. This method has a drawback in our case, since for each fixed Y , the optimal choice for Y_0 turned to be always $Y_0 \simeq Y$. However, if one blindly applies the procedure above, one gets a curve which slightly overshoots the one for the series representation with the PMS method, see Fig. 7 (right).

7. The differential cross section at the minimum $|t|$: comparison with an approach based on collinear improvement

The $\gamma^*\gamma^* \rightarrow \rho\rho$ process at the lowest order (two-gluon exchange in the t -channel) was studied in Ref. [18]. At that level our results coincide, see also [16]. The same process with the inclusion of NLA BFKL effects has been considered in Ref. [19]. In that paper, the amplitude has been built with the following ingredients: leading-order impact factors for the $\gamma^* \rightarrow \rho$ transition, BLM scale fixing for the running of the coupling in the prefactor of the amplitude (the BLM scale is found using the NLA $\gamma^* \rightarrow \rho$ impact factor calculated in Ref. [15]) and renormalization-group-resummed BFKL kernel, with resummation performed on the LLA BFKL kernel at fixed coupling [38]. In Ref. [19] the behavior of $d\sigma/dt$ at $t = t_0$ was determined as a function of \sqrt{s} for three values of the common photon virtuality, $Q = 2, 3$ and 4 GeV.

In order to make a comparison with the findings of Ref. [19], we computed $d\sigma/dt$ at $t = t_0$ for $Q = 2$ and $Q = 4$ GeV as functions of \sqrt{s} . We used $f_\rho = 216$ MeV, $\alpha_{\text{EM}} = 1/137$ and the two-loop running strong coupling corresponding to the value $\alpha_s(M_Z) = 0.12$. The results are shown in the linear-log plots of Figs. 8, which show disagreement. This is not surprising in consideration of the approximations adopted in Ref. [19],

It would be interesting to understand to what extent this disagreement is due to the use in Ref. [19] of LLA impact factors instead of the NLA ones or to the way the collinear improvement of the kernel is performed.

In order to understand to what extent the discrepancy is due to the use of leading order (LO) impact factors instead of next-to-leading order (NLO) ones, we repeated our determination of $d\sigma/dt$ at $t = t_0$ for $Q = 2$ and $Q = 4$ GeV, using LO impact factors and keeping from the their NLO contribution only the terms proportional to $\ln[s_0/(Q_1 Q_2)]$ and to $\ln[\mu_R^2/(Q_1 Q_2)]$ which are universal and needed to guarantee the s_0 - and μ_R -independence of the amplitude with NLA accuracy. The result is that $d\sigma/dt$ at $t = t_0$ increases roughly by an order of magnitude with respect to our previous determination (see Figs. 9) and therefore the disagreement with [19] becomes

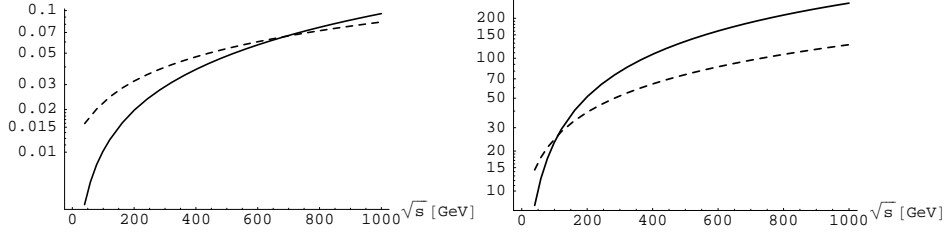


Fig. 8. Left: Linear-log plot of $d\sigma/dt|_{t=t_0}$ [pb/GeV²] as a function of \sqrt{s} at $Q^2 = 16$ GeV² ($n_f = 4$) from the series representation with the PMS optimization method (solid line) compared with the determination from the approach in Ref. [19] (dashed line). Right: The same as (left) at $Q^2 = 4$ GeV² ($n_f = 3$).

even worse. This is not surprising: impact factors give a sizable contribution to the NLA part of the amplitude which is negative with respect to the LLA part; if they are kept at LO, the NLA part of the amplitude is less negative and the total amplitude is, therefore, increased.

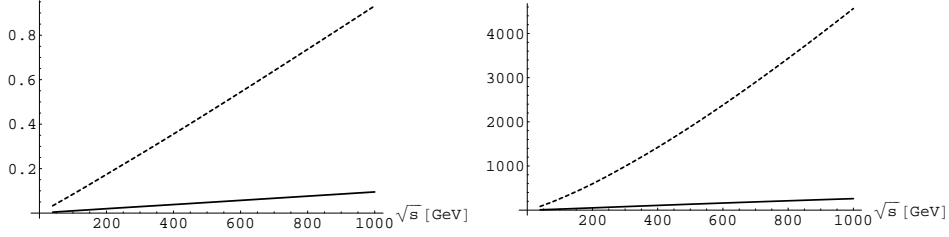


Fig. 9. Left: Linear plot of $d\sigma/dt|_{t=t_0}$ [pb/GeV²] as a function of \sqrt{s} at $Q^2 = 16$ GeV² ($n_f = 4$) from the series representation with the PMS optimization method using NLO impact factors (solid line) and LO impact factors (dashed line). Right: The same as (left) at $Q^2 = 4$ GeV² ($n_f = 3$).

8. Conclusions

We have determined the amplitude for the forward transition from two virtual photons to two light vector mesons in the Regge limit of QCD with next-to-leading order accuracy. This amplitude is the first one ever written in the next-to-leading approximation for a collision process between strongly interacting colorless particles. It is given as an integral over the ν parameter, which labels the eigenvalues of the leading order forward BFKL kernel in the singlet color representation. This form is suitable for numerical evaluations. The result obtained is independent on the energy scale s_0 , and on the renormalization scale μ_R within the next-to-leading approximation.

Using a series representation of the amplitude which includes the dependence on the energy scale and on the renormalization scale at subleading level, we performed a numerical analysis in the kinematics when the two colliding photons have the same virtuality, *i.e.* in the “pure” BFKL regime. We have found that the next-to-leading order corrections coming from the kernel and from the virtual photon to light vector meson impact factors are both large and of opposite sign with respect to the leading order contribution.

An optimization procedure, based on the principle of minimal sensitivity method, has proved to work nicely and has lead to stable results in the considered energy interval, which allows us to predict the energy behavior of the forward amplitude. The procedure consists in evaluating the amplitude at values of the energy parameters for which it is the least sensitive to variations of them. We have found that there are wide regions of values of s_0 and μ_R where the amplitude remains almost flat.

The optimal choices of s_0 and μ_R are much larger than the kinematical scales of the problem. More than being the indication of appearance of another scale in the problem, this could be related to the nature of the BFKL series. The renorm- and energy scale invariance, together with the large next-to-leading approximation corrections, call for large next-to-next-to-leading order corrections, which are most probably mimicked by unnatural optimal values for s_0 and μ_R .

The use of other optimization methods and/or different (but equivalent in the NLA) representations of the amplitude gives results does not change the behaviour of the amplitude with energy and allows for an estimate of the systematic uncertainty of our determinations.

REFERENCES

- [1] V.S. Fadin, E.A. Kuraev, L.N. Lipatov, *Phys. Lett.* **B60**, 50 (1975);
E.A. Kuraev, L.N. Lipatov, V.S. Fadin, *Zh. Eksp. Teor. Fiz.* **71**, 840 (1976)
[*Sov. Phys. JETP* **44**, 443 (1976)]; **72**, 377 (1977) [**45**, 199 (1977)];
Ya.Ya. Balitskii, L.N. Lipatov, *Sov. J. Nucl. Phys.* **28**, 822 (1978).
- [2] V.S. Fadin, L.N. Lipatov, *Phys. Lett.* **B429**, 127 (1998); M. Ciafaloni, G. Camici, *Phys. Lett.* **B430**, 349 (1998).
- [3] L.N. Lipatov, V.S. Fadin, *Sov. J. Nucl. Phys.* **50**, 712 (1989); V.S. Fadin, R. Fiore, *Phys. Lett.* **B294**, 286 (1992); V.S. Fadin, L.N. Lipatov, *Nucl. Phys.* **B406**, 259 (1993); V.S. Fadin, R. Fiore, A. Quartarolo, *Phys. Rev.* **D50**, 5893 (1994); V.S. Fadin, R. Fiore, M.I. Kotsky, *Phys. Lett.* **B359**, 181 (1995); V.S. Fadin, R. Fiore, M.I. Kotsky, *Phys. Lett.* **B387**, 593 (1996); V.S. Fadin, R. Fiore, M.I. Kotsky, *Phys. Lett.* **B389**, 737 (1996); V.S. Fadin, R. Fiore, A. Quartarolo, *Phys. Rev.* **D53**, 2729 (1996); V.S. Fadin, L.N. Lipatov, *Nucl. Phys.* **B477**, 767 (1996); V.S. Fadin, M.I. Kotsky, L.N. Lipatov, *Phys. Lett.*

- B415**, 97 (1997); V.S. Fadin, R. Fiore, A. Flachi, M.I. Kotsky, *Phys. Lett.* **B422**, 287 (1998); S. Catani, M. Ciafaloni, F. Hautmann, *Phys. Lett.* **B242**, 97 (1990); G. Camici, M. Ciafaloni, *Phys. Lett.* **B386**, 341 (1996); *Nucl. Phys.* **B496**, 305 (1997).
- [4] V.S. Fadin, [hep-ph/9807528](#).
 - [5] V.S. Fadin, R. Fiore, A. Papa, *Phys. Rev.* **D60**, 074025 (1999); V.S. Fadin, R. Fiore, A. Papa, *Phys. Rev.* **D63**, 034001 (2001); V.S. Fadin, D.A. Gorbachev, *JETP Lett.* **71**, 222 (2000); *Phys. At. Nucl.* **63**, 2157 (2000); A. Papa, [hep-ph/0107269](#).
 - [6] V.S. Fadin, R. Fiore, *Phys. Lett.* **B440**, 359 (1998).
 - [7] V.S. Fadin, R. Fiore, M.I. Kotsky, *Phys. Lett.* **B494**, 100 (2000); M.A. Braun, [hep-ph/9901447](#); M.A. Braun, G.P. Vacca, *Phys. Lett.* **B477**, 156 (2000); V.S. Fadin, R. Fiore, M.I. Kotsky, A. Papa, *Phys. Lett.* **B495**, 329 (2000); *Nucl. Phys. (Proc. Suppl.)* **99A**, 222 (2001); V.S. Fadin, A. Papa, *Nucl. Phys.* **B640**, 309 (2002); A. Papa, [hep-ph/0007118](#), [hep-ph/0301054](#); J. Bartels, V.S. Fadin, R. Fiore, *Nucl. Phys.* **B672**, 329 (2003); A.V. Bogdan, V.S. Fadin, *Nucl. Phys.* **B740**, 36 (2006); V.S. Fadin, R. Fiore, M.G. Kozlov, A.V. Reznichenko, *Phys. Lett.* **B639**, 74 (2006);
 - [8] V.S. Fadin, R. Fiore, *Phys. Lett.* **B610**, 61 (2005); Erratum **B621**, 61 (2005); *Phys. Rev.* **D72**, 014018 (2005).
 - [9] V.S. Fadin, R. Fiore, M.I. Kotsky, A. Papa, *Phys. Rev.* **D61**, 094005 (2000); *Phys. Rev.* **D61**, 094006 (2000).
 - [10] M. Ciafaloni, G. Rodrigo, *JHEP* **0005**, 042 (2000).
 - [11] J. Bartels, D. Colferai, G.P. Vacca, *Eur. Phys. J.* **C24**, 83 (2002); *Eur. Phys. J.* **C29**, 235 (2003).
 - [12] J. Bartels, S. Gieseke, C. F. Qiao, *Phys. Rev.* **D63**, 056014 (2001); Erratum **D65**, 079902 (2002); J. Bartels, S. Gieseke, A. Kyrieleis, *Phys. Rev.* **D65**, 014006 (2002); J. Bartels, D. Colferai, S. Gieseke, A. Kyrieleis, *Phys. Rev.* **D66**, 094017 (2002); J. Bartels, *Nucl. Phys. (Proc. Suppl.)* **116**, 126 (2003); J. Bartels, A. Kyrieleis, *Phys. Rev.* **D70**, 114003 (2004).
 - [13] V.S. Fadin, D.Yu. Ivanov, M.I. Kotsky, *Phys. At. Nucl.* **65**, 1513 (2002) [*Yad. Fiz.* **65**, 1551 (2002)].
 - [14] V.S. Fadin, D.Yu. Ivanov, M.I. Kotsky, *Nucl. Phys.* **B658**, 156 (2003).
 - [15] D. Yu. Ivanov, M.I. Kotsky, A. Papa, *Eur. Phys. J.* **C38**, 195 (2004); see also *Nucl. Phys. (Proc. Suppl.)* **146**, 117 (2005).
 - [16] D.Yu. Ivanov, A. Papa, *Nucl. Phys.* **B732**, 183 (2006); see also [hep-ph/0510397](#); [arXiv:0706.4392 \[hep-ph\]](#).
 - [17] D.Yu. Ivanov, A. Papa, *Eur. Phys. J.* **C49**, 947 (2007); see also *PoS DIFF2006*, 027 (2006) [[arXiv:hep-ph/0612322](#)].
 - [18] B. Pire, L. Szymanowski, S. Wallon, [hep-ph/0410108](#), *Nucl. Phys.* **A755**, 626 (2005), *Eur. Phys. J.* **C44**, 545 (2005).
 - [19] R. Enberg, B. Pire, L. Szymanowski, S. Wallon, *Eur. Phys. J.* **C45**, 759 (2006); Erratum **C51**, 1015 (2007).

- [20] B. Pire, M. Segond, L. Szymanowski, S. Wallon, *Phys. Lett.* **B639**, 642 (2006).
- [21] G.P. Salam, *J. High Energy Phys.* **9807**, 019 (1998).
- [22] F. Caporale, A. Papa, A. Sabio Vera, *Eur. Phys. J.* **C53**, 525 (2008).
- [23] F. Caporale, A. Papa, A. Sabio Vera, *Acta Phys. Pol. B* **39**, 2571 (2008), these proceedings.
- [24] V.S. Fadin, A.D. Martin, *Phys. Rev.* **D60**, 114008 (1999).
- [25] V.L. Chernyak, A.R. Zhitnitsky, *JETP Lett.* **25**, 510 (1977); *Yad. Fiz.* **31**, 1053 (1980); V.L. Chernyak, V.G. Serbo, A.R. Zhitnitsky, *JETP Lett.* **26**, 594 (1977); *Sov. J. Nucl. Phys.* **31**, 552 (1980).
- [26] G.P. Lepage, S.J. Brodsky, *Phys. Lett.* **B87**, 359 (1979); *Phys. Rev. Lett.* **43**, 545 (1979); Erratum **43**, 1625 (1979); *Phys. Rev.* **D22**, 2157 (1980); S.J. Brodsky, G.P. Lepage, A.A. Zaidi, *Phys. Rev.* **D23**, 1152 (1981).
- [27] A.V. Efremov, A.V. Radyushkin, *Phys. Lett.* **B94**, 245 (1980); *Teor. Mat. Fiz.* **42**, 147 (1980).
- [28] P. Ball, V.M. Braun, Y. Koike, K. Tanaka, *Nucl. Phys.* **B529**, 323 (1998).
- [29] I.F. Ginzburg, D.Yu. Ivanov, *Phys. Rev.* **D54**, 5523 (1996).
- [30] S.J. Brodsky, V.S. Fadin, V.T. Kim, L.N. Lipatov, G.B. Pivovarov, *JETP Lett.* **76**, 249 (2002).
- [31] S.J. Brodsky, V.S. Fadin, V.T. Kim, L.N. Lipatov, G.B. Pivovarov, *JETP Lett.* **70**, 155 (1999).
- [32] P.M. Stevenson, *Phys. Lett.* **B100**, 61 (1981); *Phys. Rev.* **D23**, 2916 (1981).
- [33] G. Racah, *Nuovo Cim.* **14**, 93 (1937).
- [34] G. Grunberg, *Phys. Lett.* **B95**, 70 (1980); Erratum **B110**, 501 (1982); **B114**, 271 (1982); *Phys. Rev.* **D29**, 2315 (1984).
- [35] J. Bartels, M. Lublinsky, *Mod. Phys. Lett.* **A19**, 19691982 (2004).
- [36] M. Ciafaloni, D. Colferai, *Phys. Lett.* **B452**, 372 (1999); M. Ciafaloni, D. Colferai, G.P. Salam, *Phys. Rev.* **D60**, 114036 (1999), *JHEP* **9910**, 017 (1999), *JHEP* **0007**, 054 (2000); M. Ciafaloni, D. Colferai, G.P. Salam, A.M. Stasto, *Phys. Lett.* **B576**, 143 (2003), *Phys. Rev.* **D68**, 114003 (2003); G. Altarelli, R.D. Ball, S. Forte, *Nucl. Phys.* **B575**, 313 (2000); *Nucl. Phys.* **B599**, 383 (2001); *Nucl. Phys.* **B621**, 359 (2002); *Nucl. Phys.* **B674**, 459 (2003); R.S. Thorne, *Phys. Rev.* **D60**, 054031 (1999); *Phys. Lett.* **B474**, 372 (2000); *Phys. Rev.* **D64**, 074005 (2001); A. Sabio-Vera, *Nucl. Phys.* **B722**, 65 (2005); R. Peschanski, C. Royon, L. Schoeffel, *Nucl. Phys.* **B716**, 401 (2005).
- [37] S.J. Brodsky, G.P. Lepage, P.B. Mackenzie, *Phys. Rev.* **D28**, 228 (1983).
- [38] A. Khoze, A.D. Martin, M.G. Ryskin, W.J. Stirling, *Phys. Rev.* **D70**, 074013 (2004); hep-ph/0406135.